

# Alignment-Free, Self-Calibrating Elbow Angles Measurement using Inertial Sensors

Philipp Müller<sup>1</sup>, Marc-André Bégin<sup>2</sup>, Thomas Schauer<sup>1</sup> and Thomas Seel<sup>1</sup>

**Abstract**—Due to their relative ease of handling and low-cost, inertial measurement unit (IMU) based joint angle measurements are used for a widespread range of applications. These include sports performance, gait analysis and rehabilitation (e.g. Parkinson’s disease monitoring or post-stroke assessment). However, a major downside of current algorithms recomposing human kinematics from IMU data is that they require calibration motions and/or the careful alignment of the IMUs respective to their body segment. In this article, we propose a new method, which is alignment free and self-calibrated using the arbitrary movements of the user and an initial zero reference arm pose. The proposed method utilizes real time optimization to identify the two dominant axes of rotation of the elbow joint. Using a two degree of freedom joint mimicking the human elbow, the performance of the algorithm was assessed by comparing the angles obtained from two IMUs to the ones obtained from a marker-based optical tracking system. The self-calibration proved to converge within seconds and the RMS errors with respect to the optical reference system were below 5°. Our method can be particularly useful in the field of telerehabilitation, where precise manual sensor to segment alignment as well as precise, predefined calibration movements are impractical.

**Index Terms**—Elbow tracking, two degree of freedom (2DOF) joint, upper limb motion, inertial measurement units (IMU)

## I. INTRODUCTION

Longtime considered as the gold standard in the field of human motion measurements for their high degree of accuracy, optical tracking systems have proven to be poor candidates in such areas as the remote follow up on training schemes for patient rehabilitation due to their low mobility, complex setup and high cost. For such applications where it is impractical for human subjects to travel to specialized laboratories equipped with optical measurement systems, inertial measurement units (IMUs) are preferred over exoskeletons and goniometers because the latter tend to restrict natural motion of the patient and the cost of the former remains low in comparison [1], [2]. In general, an IMU fuses the information provided by a multi-axis accelerometer and a multi-axis gyroscope in order to infer the position and orientation of the sensor by integration [3], [4]. To compensate for measurement drifts inherent to IMUs, some commercially available systems incorporate a magnetometer to the design in which case the relative orientation of the IMU can be known with respect to the world reference frame.

From the absolute orientation of two IMUs placed on two different body segments forming a joint (e.g. the elbow joint), the angles of this joint can be inferred by decomposing the relative orientation between both IMUs along the rotation axes of the joint. This process requires however the orientation of the joint rotation axes to be known in each of the IMUs reference frames. As of now, this has been done using either careful alignments [5]–[7] and identification of relevant body landmarks recommended by the International Society of Biomechanics [8] or by using a set of predefined and precisely carried out calibration motions [9]–[12]. The purpose of this paper is to propose a new algorithm for calculating the relative orientation of the elbow which does not depend on sensor alignment nor calibration procedures, but self-calibrates online from the arbitrary movements of the user. This algorithm uses the kinematic constraints of the elbow to estimate the dominant axes of rotation of the joint expressed in each IMU reference frame, similarly to what has been done previously for the knee joint [13]. The method is tested on an idealized mechanical elbow using two IMUs. Then the estimates of the new algorithm are compared to the angle measurements provided by an optical marker-based tracking system.

## II. METHOD

### A. Design of the Algorithm

Our method is based on the addition theorem for angular velocities. The relative angular velocity of two objects can be decomposed into a sum of angular velocities around different rotation axes; thus if the two correct rotation axes of the elbow are found, the relative angular velocity has to be a linear combination of the two.

By neglecting the carrying angle, the human elbow can be modeled as a two-dimensional joint connecting two segments where the two dimensions represent the flexion/extension (FE) and the pronation/supination (PS) axes of the elbow [8]. Given two IMUs where IMU1 is in frame A and attached to segment 1 and IMU2 is in frame B and attached to segment 2 (see Fig. 1), then the relative angular velocity of the elbow in the frame of IMU1 is

$$\boldsymbol{\omega}_r^A = -\boldsymbol{\omega}_{\text{IMU1}}^A + \mathbf{R}_A^B \boldsymbol{\omega}_{\text{IMU2}}^B, \quad (1)$$

where  $\boldsymbol{\omega}_{\text{IMU1}}^A$  and  $\boldsymbol{\omega}_{\text{IMU2}}^B$  are the angular velocities measured by IMU1 and IMU2, respectively and  $\mathbf{R}_A^B$  is the relative IMU orientation which can be obtained from the two estimated absolute IMU orientations.

For a joint with two rotational degrees of freedom around the unit axis  $\mathbf{a}^A$  in the frame of IMU1 and  $\mathbf{b}^B$  in the frame

Control Systems Group (Fachgebiet Regelungssysteme), Technische Universität Berlin, 10623 Berlin, Germany  
Mueller@control.TU-Berlin.de  
Schauer@control.TU-Berlin.de  
Seel@control.TU-Berlin.de

Université de Sherbrooke, 2500, boul. de l’Univ., Sherbrooke, Canada  
Marc-Andre.Begin@USherbrooke.ca

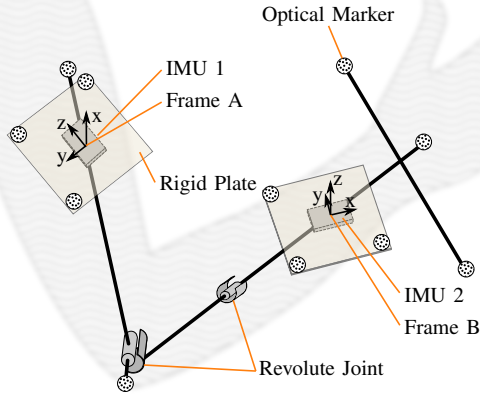


Fig. 1: Representation of the mechanical device resembling the human elbow joint. Shown are the two revolute joints, the two IMUs and the optical markers.

of IMU2, the relative angular velocity can be expressed as

$$\boldsymbol{\omega}_r^A = \alpha \mathbf{a}^A + \beta \mathbf{R}_A^B \mathbf{b}^B + \mathbf{e}, \quad (2)$$

where  $\alpha$  and  $\beta$  are scalars and  $\mathbf{e}$  expresses the error in the case that  $\mathbf{a}^A$ ,  $\mathbf{b}^B$ ,  $\alpha$  or  $\beta$  are not known perfectly.

For every given approximated values of  $\mathbf{a}^A$ ,  $\mathbf{b}^B$  and  $\mathbf{R}_A^B$ , the factors  $\alpha$  and  $\beta$  can be found such that  $\mathbf{e}$  is minimal. In this case, the vector  $\mathbf{e}$  stands normal to the plane that is spanned by  $\mathbf{a}^A$  and  $\mathbf{R}_A^B \mathbf{b}^B$ . The magnitude of this minimal error can then be expressed as

$$e = \frac{\boldsymbol{\omega}_r^A \cdot (\mathbf{a}^A \times (\mathbf{R}_A^B \mathbf{b}^B))}{\|\mathbf{a}^A \times (\mathbf{R}_A^B \mathbf{b}^B)\|_2}. \quad (3)$$

When measurements of multiple points in time are available, the squared errors of each measurement can be summed into one cost function defined as

$$J(\mathbf{a}^A, \mathbf{b}^B) = \sum_{k=1}^N e_k^2. \quad (4)$$

A local minimum of this nonlinear function can be found by using optimization techniques such as the gradient descent algorithm. For this class of methods, the gradient  $\frac{\partial J}{\partial (\mathbf{a}^A, \mathbf{b}^B)}$  has to be determined. The unit vector properties of  $\mathbf{a}^A$  and  $\mathbf{b}^B$  allow a two parameter expression in spherical coordinates. Hence  $\frac{\partial J}{\partial \boldsymbol{\phi}}$  can be used instead, where  $\boldsymbol{\phi}$  is a four dimensional vector containing the spherical coordinate parameters of the two axis. The analytical gradient expression can be obtained using differential calculus.

For the sake of real time capability, a window of measurements is chosen such that the cost function is calculated for the last  $M$  measurements. With each new measurement, the window is shifted by one time step and a new gradient descent step is executed.

The last step is to calculate the joint angles from the estimated axes and the relative orientation of the two IMUs. The two estimated rotation axes are possibly non orthogonal. This can be the case when the solution did not yet converge or

when the mechanical joint is non orthogonal. A generalized Euler decomposition was used to extract the two joint angles along arbitrary axes [14].

At a defined point in time, a "zero pose" (e.g. straight arm) has to be performed; thus, defining the obtained joint angles to be zero at this arm position. The relative IMU orientation of this pose is stored and with each update of the estimated axes, the current angle offset is calculated using the generalized Euler decomposition. The resulting offset is then subtracted from the calculated angles. Accordingly, the offset for the optical reference angles is also obtained from the "zero pose".

## B. Experimental Setup

A mechanical setup (Fig. 1) replicating the human elbow joint was chosen for the experimental verification. The IMUs were placed such that each rotation axis corresponded to one of the IMUs principal axis. This alignment is not required to obtain accurate angles. However, it established a reference to which the estimated axes could be later compared. The z-axis of IMU1 was aligned with the FE axis and the x-axis of IMU2 with the PS axis. The used IMUs were Xsens MTw wireless units (Xsens Technologies B.V., Netherlands).

On the human arm, the IMUs have to be attached to the skin, which leads to position and orientation errors known as skin movement artifacts. To emulate this behavior, a layer of soft rubber foam was added between each IMU and the mechanism using hook and loop fastener tape. Two experiments were conducted; a first one without foam and then a second one with the rubber foam layer.

Here, a Vicon optical marker measurement system (Vicon Motion Systems Ltd. UK) was chosen as a reference in order to verify the IMU based angle measurement. For this, the mechanical device was equipped with optical markers (Fig. 1). In order to quantify the emulated skin movement artifacts, markers were also attached to the IMUs directly by using rigid plates. The simple geometrical relations of the optical markers and the mechanism were then used to calculate the joint angles and the emulated skin movement artifacts from the 3D trajectories of the markers.

During the experiment, the device was first held approximately still in the hands of the assistant at a defined position for ten seconds. The "zero pose" was set in the middle of this still period. Then, both axis were excited at approximately 1 Hz while the device was randomly rotated and displaced at a slow rate for 30 seconds. The slow random movement of the device was used to emphasize the immunity of the algorithm to absolute movements of the IMUs.

Two sets of reference joint angles were obtained, one IMU based and one optical based reference. The IMU based reference joint angles resulted from using the axis expected from the IMU alignment together with the IMU orientation data.

For both experiments the exact same set of parameters was used, including the parameterization of the gradient descent algorithm.

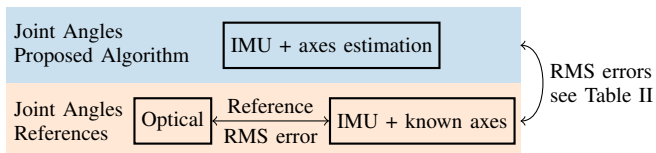


Fig. 2: The three sets of angles that are obtained for each experiment. The two reference angles are compared to the angles of the proposed algorithm as well as to each other.

TABLE I: Evaluation of the emulated skin movement artifacts, showing the RMS values of the rotation as well of the absolute translation. In experiment 2, additional IMU movement was enabled by adding a rubber foam layer.

		Roll	Pitch	Yaw	Absolute Translation
Experiment 1	IMU1	1.21°	1.24°	1.64°	2.55 mm
	IMU2	1.33°	1.31°	1.54°	1.45 mm
Experiment 2	IMU1	4.43°	4.14°	6.32°	3.63 mm
	IMU2	3.56°	3.74°	3.25°	2.60 mm

### III. RESULTS

All RMS values presented in this section were obtained from a window spanning from 10s to 30s after the start of the motion, which meant full convergence of the algorithm.

The movement of the two IMUs with respect to the segments was quantified for both experiments and is presented in Table I.

As illustrated in Fig. 2 the angles obtained by the proposed algorithm were compared to the two sets of reference angles. Additionally, the references were compared against each other.

The estimated axes using the proposed algorithm for both experiments (without and with the skin motion emulation) are presented in Fig. 3 and Fig. 4. Note that the origin of the time axis is placed at the start of the excitation motion. During the prior 10s, the device is held still by the assistant.

First, both references were compared against each other, as depicted in Fig. 2. The resulting RMS errors for the first experiment were 2.29° for the FE angle and 5.79° for the PS angle. For the second experiment, the errors were 9.17° and 13.41°, respectively.

Subsequently, the joint angles measured with the proposed method were compared to both references. The resulting

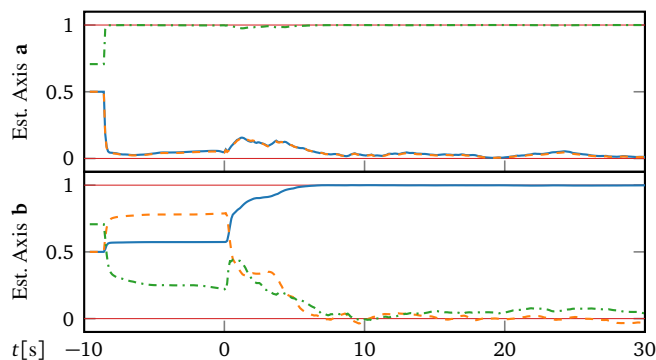


Fig. 3: The estimated axes of rotation of the mechanical device  $x$  (—),  $y$  (---) and  $z$  (-.-) and the expected constant axes values (—). The motion is started at 0s. In this experiment, the IMUs are rigidly attached to the mechanism.

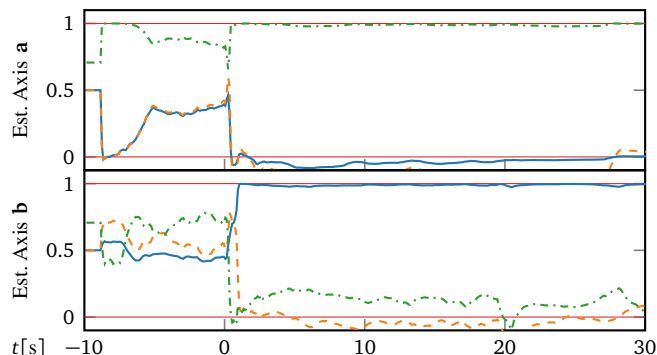


Fig. 4: The estimated axes of rotation of the mechanical device  $x$  (—),  $y$  (---) and  $z$  (-.-) and the expected constant axes values (—). In the second experiment the IMUs are placed on a layer of rubber foam to emulate skin motion.

TABLE II: RMS errors of the joint angles comparing the joint angles acquired by the IMU measurements together with the estimated axes with the IMU based angles using the correct axes and the angles provided by the optical reference for A) rigid mounting of the IMUs and B) with the skin motion emulation. The RMS value was calculated from 10s after the start of the movement up to 30s after.

		IMU reference	Optical reference
A)	Flexion/extension	1.86°	3.32°
	Pronation/supination	2.02°	4.75°
B)	Flexion/extension	2.75°	10.14°
	Pronation/supination	5.30°	11.46°

RMS errors are presented in Table II. In Fig. 5 the angles obtained with the proposed method are shown together with the optical reference angles for the first experiment. The first 10 seconds of the experiment during which a large error is observed correspond to the time of convergence of the rotation axis  $b$  as shown in Fig. 3.

### IV. DISCUSSION

The proposed method allows the user to mount the IMUs on both arm segments in an arbitrary orientation. Given that the arbitrary movements of the user contain both FE and PS, the self-calibration is complete within seconds and the correct angles are measured.

The results showed that for both experiments, the algorithm was able to converge towards the true PS and FE axes.

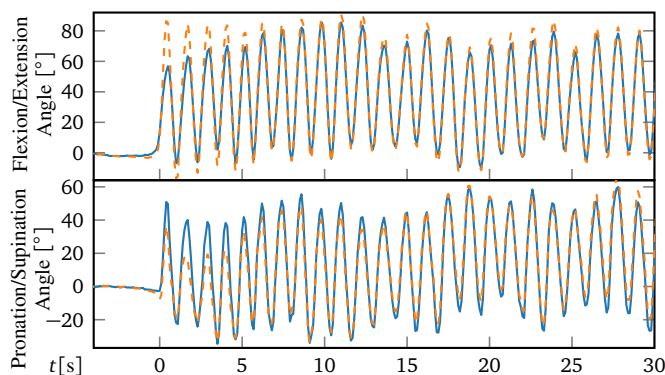


Fig. 5: Flexion/extension angle acquired by the optical reference measurement (—) and by using the IMU measurements together with the estimated axes (---). Correspondingly the pronation/supination angle is presented.

In the first experiment, the FE axis already converged before the movement of the device was initiated. This means that the minor involuntary movements originating from the assistant holding the device were sufficient to estimate this axis. The PS axis on the contrary converged only after approximately 5 s of excitation. The second experiment with the emulated skin motion was expected to be much more challenging for the algorithm, since a movement around a wrong axis can lead the gradient descent in a wrong direction (using the moving window). This problem can be addressed by reducing the step size. A small step size limits the harm of a step in the wrong direction. Despite these challenges, a fast and smooth convergence to the correct axis was achieved for both axes.

The mechanical setup allowed us to evaluate the skin motion artifacts in IMU based angle measurements. The results showed that even with a perfectly known alignment of the IMUs, the emulated skin motion lead to RMS errors between  $9^\circ$  and  $13^\circ$ .

Using the proposed method, the joint angles could be measured accurately as soon as the algorithm converged. The RMS errors with respect to the optical reference were between  $3^\circ$  and  $5^\circ$  for the first experiment. With the emulated skin motion the RMS errors fell in the exact same range as the RMS errors for the perfectly known IMU alignment. Other studies have evaluated their IMU based 2DOF angle measuring algorithms on mechanical devices and on the human body. For tests led on mechanical devices using rotational encoders, typical RMS errors varied between  $1^\circ$  and  $4^\circ$  depending on the method used and on the speed of motion which lies within the range of RMS errors obtained through the proposed algorithm [15], [16]. For tests led on actual human elbows, the typical RMS error range stretches up to  $5^\circ$  for slow arm motions at about  $45^\circ/\text{s}$  around the FE axis for instance [2], [5]. Assuming that the experiments led with the IMUs bounded by foam to the mechanical structure successfully replicates the skin motion effect observed with human segments, the RMS error on the results obtained through our method are about twice as large. The tests however were conducted at speeds generally twice as large (about  $90^\circ/\text{s}$  around the FE axis) and it could also be that the elasticity of the foam was overestimated. In all cases, more tests would need to be done on human subjects.

## V. CONCLUSION

A method that allows the determination of joint angles without the need of specific IMU alignment was developed. The method is self-calibrated by estimating two elbow joint axes online, therefore specific calibration movements are not necessary except for the definition of a zero reference. A mechanical device which resembles the human elbow joint and emulates the skin motion was built and used along with an optical marker-based tracking system to evaluate the performance of the method.

The method proved to be robust enough to deal with the disturbances of skin motion and was able to converge within seconds to the correct joint axes. When comparing the angle tracking accuracy with those of other IMU based

elbow tracking methods (which all need either careful sensor alignment or predefined calibration movements), our new method proved to be competitive.

Further studies will most importantly address the performance on the human subject. This should be done with healthy subjects as well as in a rehabilitation setting. Additionally an analytical proof of convergence of the algorithm will be addressed.

## ACKNOWLEDGMENT

We thank our colleagues of the Fraunhofer IKP (Pascalstraße 8-9, 10587 Berlin, Germany) for supplying the optical measurement system and helping us with the measurements.

## REFERENCES

- [1] C. Wong, Z.-q. Zhang, B. Lo, and G.-Z. Yang, "Wearable Sensing for Solid Biomechanics: A Review," *IEEE Sensors Journal*, vol. 15, pp. 2747–2760, May 2015.
- [2] H. Zhou, T. Stone, H. Hu, and N. Harris, "Use of multiple wearable inertial sensors in upper limb motion tracking," *Medical Engineering & Physics*, vol. 30, pp. 123–133, Jan. 2008.
- [3] I. Prayudi and D. Kim, "Design and implementation of IMU-based human arm motion capture system," in *2012 International Conference on Mechatronics and Automation (ICMA)*, pp. 670–675, Aug. 2012.
- [4] G. Welch and E. Foxlin, "Motion tracking survey," *IEEE Computer Graphics and Applications*, pp. 24–38, 2002.
- [5] A. G. Cutti, A. Giovanardi, L. Rocchi, A. Davalli, and R. Sacchetti, "Ambulatory measurement of shoulder and elbow kinematics through inertial and magnetic sensors," *Medical & Biological Engineering & Computing*, vol. 46, pp. 169–178, Dec. 2007.
- [6] P. Picerno, A. Cereatti, and A. Cappozzo, "Joint kinematics estimate using wearable inertial and magnetic sensing modules," *Gait & Posture*, vol. 28, pp. 588–595, Nov. 2008.
- [7] J.-T. Zhang, A. C. Novak, B. Brouwer, and Q. Li, "Concurrent validation of Xsens MVN measurement of lower limb joint angular kinematics," *Physiological Measurement*, vol. 34, no. 8, p. N63, 2013.
- [8] G. Wu, F. C. T. van der Helm, H. E. J. (DirkJan) Veeger, M. Makhssous, P. Van Roy, C. Anglin, J. Nagels, A. R. Karduna, K. McQuade, X. Wang, F. W. Werner, and B. Buchholz, "ISB recommendation on definitions of joint coordinate systems of various joints for the reporting of human joint motion-Part II: shoulder, elbow, wrist and hand," *Journal of Biomechanics*, vol. 38, pp. 981–992, May 2005.
- [9] W. S. Ang, I.-M. Chen, and Q. Yuan, "Ambulatory measurement of elbow kinematics using inertial measurement units," in *2013 IEEE/ASME International Conference on Advanced Intelligent Mechatronics (AIM)*, pp. 756–761, July 2013.
- [10] W. H. K. de Vries, H. E. J. Veeger, A. G. Cutti, C. Baten, and F. C. T. van der Helm, "Functionally interpretable local coordinate systems for the upper extremity using inertial & magnetic measurement systems," *Journal of Biomechanics*, vol. 43, pp. 1983–1988, July 2010.
- [11] H. J. Luinge, P. H. Veltink, and C. T. M. Baten, "Ambulatory measurement of arm orientation," *Journal of Biomechanics*, vol. 40, no. 1, pp. 78–85, 2007.
- [12] L. Ricci, D. Formica, L. Sparaci, F. R. Lasorsa, F. Taffoni, E. Tamilia, and E. Guglielmelli, "A New Calibration Methodology for Thorax and Upper Limbs Motion Capture in Children Using Magneto and Inertial," *Sensors*, vol. 14, pp. 1057–1072, Jan. 2014.
- [13] T. Seel, T. Schauer, and J. Raisch, "Joint axis and position estimation from inertial measurement data by exploiting kinematic constraints," in *2012 IEEE International Conference on Control Applications (CCA)*, pp. 45–49, Oct. 2012.
- [14] G. Piovan and F. Bullo, "On Coordinate-Free Rotation Decomposition: Euler Angles About Arbitrary Axes," *IEEE Transactions on Robotics*, vol. 28, pp. 728–733, June 2012.
- [15] M. El-Gohary and J. McNames, "Human Joint Angle Estimation with Inertial Sensors and Validation with A Robot Arm," *IEEE Transactions on Biomedical Engineering*, vol. 62, pp. 1759–1767, July 2015.
- [16] K. Hirose, H. Doki, and A. Kondo, "A measurement method of the 2dof joint angles and angular velocities using inertial sensors," in *2012 Proceedings of SICE Annual Conference (SICE)*, pp. 366–371, Aug. 2012.